Machine Learning for Recognition and Mapping of Rare Earths in Brazil using Reflectance Spectroscopy and Hyperspectral Imagery

Matheus M. Gomes[1], Ruy M. Castro[2], Gustavo S. Vieira[3]

[1]Aeronautics Institute of Technology, São José dos Campos, Brazil – matheus.mmg@ita.br
[2]Institute for Advanced Studies, São José dos Campos, Brazil – ruyrmc@fab.mil.br
[3]Institute for Advanced Studies, São José dos Campos, Brazil – gustavogsv@fab.mil.br

Keywords: Machine Learning, Rare Earth Elements, Recognition, Mapping, Reflectance spectroscopy, Hyperspectral imagery.

Abstract

Rare Earth Elements are fundamental to the global technology industry. Found in various rocks and soils, the elements that compose them are the raw material for the production of components that are incorporated into a wide range of applications, from household appliances to aircraft, and therefore it is relevant to identify and map them in an automated way, through Artificial Intelligence. In this context, reflectance spectroscopy is capable of providing the important data for the eventual identification of soils, rocks and minerals, and, in conjunction with images from hyperspectral sensors onboard satellite or airborne platforms, it is also possible to map the regions where these elements occur. This work measured the reflectance spectra of soil and rock samples containing Rare Earth Elements from the Poços de Caldas region, a municipality in the state of Minas Gerais, Brazil. The measured spectra were used as input data for a classification neural network, which compared them with spectra captured by the hyperspectral sensor of the PRISMA Satellite.

1. Introduction

According to the International Union of Pure and Applied Chemistry (IUPAC), Rare Earth Elements (REE) are defined as a set of 17 chemical elements that include: the lanthanide series, yttrium, and scandium (Lapido-Loureiro, 2013). These elements and their oxides exhibit unique electrical and magnetic properties, making them essential for the high-tech industry and the energy transition.

These elements are found in various soils, minerals, and rocks present in the Earth's crust, and can eventually be identified through their reflectance spectra, measured in the laboratory or detected by orbital imaging sensors.

Reflectance spectra in the visible and shortwave infrared (SWIR) ranges, which are part of the optical range of the electromagnetic spectrum, act as a spectral signature of the material, enabling its identification through diagnostic absorption bands.

In the laboratory or in the field, a spectroradiometer is the equipment capable of measuring the reflected radiant flux, relative to a reference surface, and recording the spectral curve of the target.

With the evolution of Artificial Intelligence (AI), different Machine Learning techniques have been applied to recognize materials through their spectra, enabling the mapping of targets from different platforms, such as airborne and orbital ones.

This work proposes the use of an Artificial Neural Network (ANN) to identify rocks, soils, and rare earth minerals in Brazilian territory through their spectral signatures, measured in the Laboratory of Radiometry and Characterization of Electro-optical Sensors (LaRaC), located in São José dos Campos, Brazil, and the mapping of their occurrences using images captured by the hyperspectral sensor of the PRISMA Satellite, obtained from a public collection made available by the Italian Space Agency (ASI).

2. Rare Earth Elements

Despite their name, some REE are very common in the Earth's crust, even more so than silver and mercury, for example (Moraes and Seer, 2018). They receive this name due to the difficulty of extracting and chemically separating them from the rocks of origin, a long and costly process.

REE can be divided into groups by density, as shown in Table 1. According to Abrão (1994), Rare Earth Elements with even atomic numbers are more abundant than those with odd atomic numbers, a result of greater nuclear stability associated with even numbers of protons.

Group	Element	Symbol	Z
Light	Lanthanum	La	57
	Cerium	Ce	58
	Praseodymium	Pr	59
	Neodymium	Nd	60
	Promethium	Pm	61
Medium	Samarium	Sm	62
	Europium	Eu	63
	Gadolinium	Gd	64
Heavy	Terbium	Tb	65
	Dysprosium	Dy	66
	Holmium	Ho	67
	Erbium	Er	68
	Thulium	Tm	69
	Ytterbium	Yb	70
	Lutetium	Lu	71
	Yttrium	Y	39
	Scandium	Sc	21

Table 1. Groups of REE in relation to density.

This contribution has been peer-reviewed.

These elements are characterized by being ductile, malleable, and highly magnetizable, and therefore are fundamental raw materials in the electronics and automotive industries.
Brazil is the second largest holder of rare earth reserves in the world, with approximately 22 million tons, second only to China, which occupies the first position with 44 million tons (Heider and Siqueira, 2025).

In Brazilian territory, rare earths are found mainly in the monazite sands of the coast and in deposits near extinct volcanoes, but unexplored reserves are known to exist in the Amazon region.

Lapido-Loureiro (2013) explains that Brazil's great potential for REE is based on the plurality of their occurrences, the multiplicity of their geological environments, and their geographical dispersion.

However, the mapping of these elements in the country is still low. According to data from the Mineral Resources Research Company (CPRM), only 28% of Brazilian geology has been mapped at a scale of 1:100,000, the so-called detailed scale, as can be seen in Figure 1, which highlights an important gap in national geological knowledge (Cabral Neto et al, 2026).

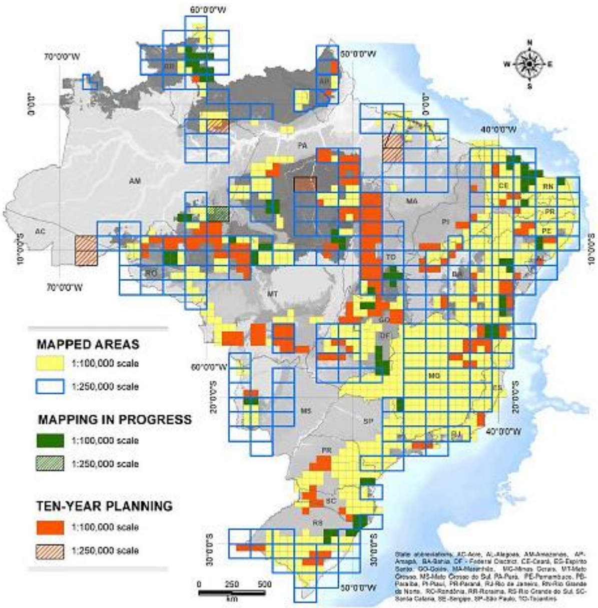

Figure 1. Status of geological mapping of Brazil (Cabral Neto et al, 2026).

According to CPRM, the expansion of Brazilian geological mapping is fundamental to attract investments in mineral exploration and discover new deposits (Cabral Neto et al, 2026). Furthermore, geological mapping also serves as a basis for other activities, such as water resource management, environmental evolution studies, and territorial planning.

The state of Minas Gerais (MG) stands out for containing a large and diverse alkaline complex, especially in the region near the municipality of Poços de Caldas (Lapido-Loureiro, 2013). Therefore, regolith samples from this region, containing different concentrations of REE, were obtained to measure their reflectance factors in the laboratory.

A review by Goodenough et al (2021) showed that many of the world's most important REE deposits are found in alkaline carbonatite complexes, such as Eden Lake in Canada and Mountain Pass in the United States.
The samples are shown in Figure 2 and consist of regolith derived from three types of alkaline rocks: phonolite, tinguaite, and nepheline syenite.

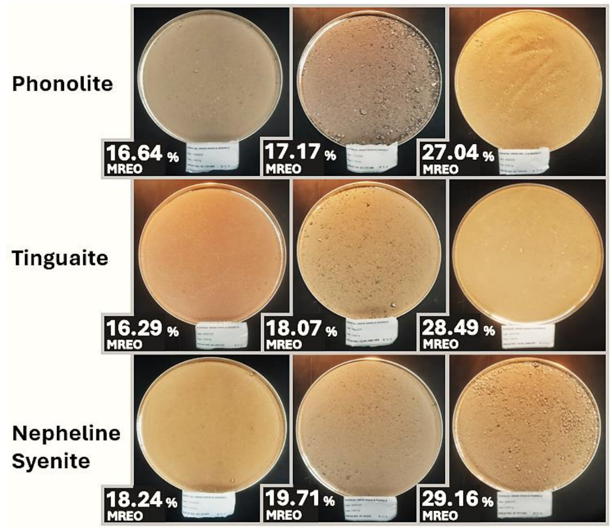

Figure 2. Regolith samples from alkaline rocks with Rare Earth Elements from Poços de Caldas/MG.

The samples contain different concentrations of Rare Earth Oxides (REO), predominantly Medium Rare Earth Oxides (MREO). Samples with MREO greater than 27% have medium REE ranging from 20 to 100 ppm, while those with lower concentrations range from 4 to 21 ppm.

3. Remote sensing for rocks and soils analysis

At room temperature, most objects are visible not by the radiation they emit, but by the radiation they reflect. This is how remote sensing is mostly done, by detecting and quantitatively measuring the interaction of electromagnetic radiation with a specific target, enabling data collection without physical contact with the material (Meneses, Almeida and Baptista, 2019).

Measurements can be performed on different platforms, such as aerial, with the sensor attached to airplanes or drones; orbital, with the sensor mounted on imaging satellites; and even in the laboratory, using spectroscopy equipment.

Spectroscopy can provide important information about different materials. In soils and rocks, measured reflectance is relevant for various geological studies, allowing the identification of minerals that make up the target and providing information about its chemical composition.

Abrão (1994) explains that the spectrographic method is very useful, but has limitations for the determination of an individual rare earth element in the complex mixture in which all the elements are present, making it difficult to locate a line free of interference.

However, it is possible to identify certain characteristics of the rock and the presence of some minerals through the absorption bands presented.

This is because, physically, it is known that electromagnetic radiation does not have the ability to penetrate the minerals of the rock, limiting its interaction to the first 50 µm, making it possible to identify only the minerals that are on the surface (Meneses, Almeida and Baptista, 2019).

The absorption band, sometimes called diagnostic absorption, represents the wavelengths that most affect a given oxide or mineral. Therefore, the features of the curve indicate the chemical composition of the rock or soil.

Figure 3 shows the spectra measured at LaRaC of phonolite regolith samples, which is an extrusive igneous rock of intermediate chemical composition, considered to be the fine-grained nepheline syenite (Sgarbi et al, 2007).

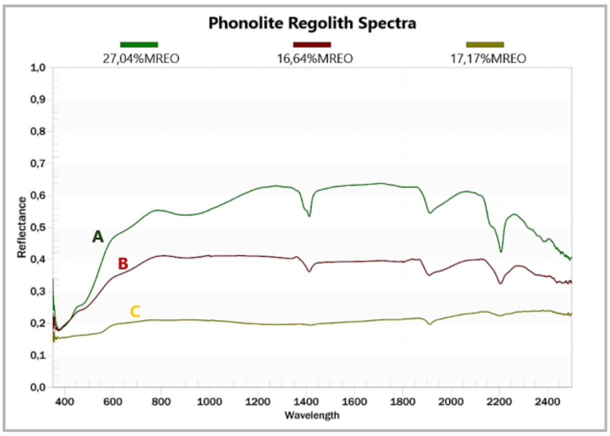

Figure 3. Spectra measured at LaRaC of the Phonolite samples.

As is the case of a surface measurement, the shape of the spectra is influenced by the iron oxides present in the composition of the samples, which exhibit absorptions centered at 500 nm, 700 nm, and 900 nm, as can be clearly seen in samples A and B.

The flatness of the spectrum of sample C points to the presence of opaque minerals, causing the water absorption bands, near 1400 and 1900 nm, to become very weak.

The broad absorption band around 1000 nm indicates that sample A belongs to the ultrabasic rock category, which is confirmed by the presence of silica in the sample, at 39.53%. Samples B and C have less intense absorption bands, which is characteristic of intermediate rocks, as confirmed by the amount of silica, which represents 53.00% and 53.94% in samples B and C, respectively.

The intense, double bands centered at 1400 and 2200 nm in sample A indicate the presence of the mineral kaolinite. Observing the same bands in sample B, they are intense but simple, suggesting the predominance of the mineral montmorillonite. In the case of sample C, these bands are weak and simple, which may point to the presence of the mineral illite.

Kaolinite absorption bands are present in all spectra of samples with an MREO composition greater than 27%, as can be seen in Figure 4.

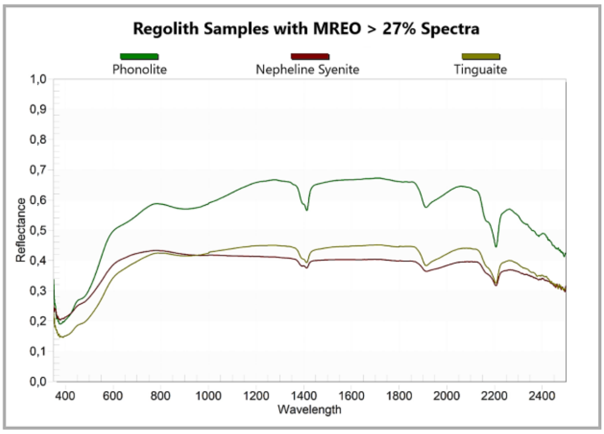

Figure 4. Spectra measured at LaRaC of samples with an MREO composition greater than 27%.

Although some rock spectra that typically contain REE are available in open spectral libraries, there is still not a wide variety of measurements, neither a library dedicated to these elements and minerals.

As reported by Bedini (2017), some studies have analyzed spectra of carbonatite samples, which are an important source of rare earth elements, but there are still no large-scale remote sensing studies on these elements.

Therefore, compiling a comprehensive spectral database that includes soils, rocks, and rare earth minerals is relevant, enabling future remote sensing and mineral prospecting work.

4. Hyperspectral images from the PRISMA Satellite

The PRISMA Satellite is positioned in Low Earth Orbit (LEO), 615 km from Earth, with a 29-day repeating cycle. Its payload consists of a hyperspectral imaging sensor, capable of capturing images in a spectral range of 400 to 2500 nm, as well as a medium-resolution panchromatic camera (Italian Space Agency, 2020).

Each hyperspectral image represents an area of 900 km², where each pixel has a Ground Sample Distance (GSD) of 30 m. The images captured by the satellite are processed and made available in an online repository, where radiance and reflectance products can be obtained directly.

Genú and Demattê (2012) explain that when moving from terrestrial to orbital levels, spectral resolution decreases, but it is still possible to analyze the orbital spectral response through the reflectance intensity of the curves.

Badura and Dąbski (2022) also point out that hyperspectral images can be used to efficiently map a deep weathering front, such as regolith, and also serve as a basis for soil studies and precision agriculture.

In this work, an orthorectified hyperspectral image captured by PRISMA Satellite on October 20, 2025, of the Poços de Caldas region, located in the South/Southwest of the state of Minas Gerais, as shown in Figure 5, was analyzed. Mataveli and Morato (2011) studied the urban expansion of the municipality of Poços de Caldas, and pointed out its environmental applications through remote sensing.

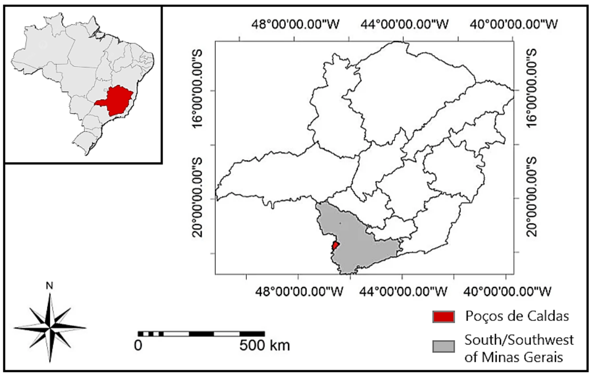

Figure 5. Location of the Poços de Caldas region. (Adapted from Mataveli and Morato, 2011)

The PRISMA Product used is of the L2C type, which already provides surface reflectance, and therefore, atmospheric corrections are not necessary.

Figure 6 shows a comparison between the spectrum of one of the tinguaite samples measured in the laboratory and the surface reflectance spectrum captured by the PRISMA satellite in a mining area. Both spectra present key diagnostic features that indicates a high degree of similarity.

Reflectance values recorded by PRISMA below 0.055 were discarded because they generally represent noise inherent to the sensor or the environment.

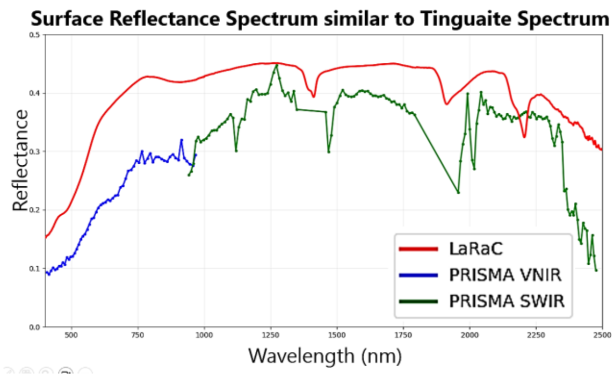

Figure 6. Comparison between spectrum measured at LaRaC and spectrum captured by the PRISMA Satellite.

It is noted that both spectra exhibit their highest reflectance value at the same point, at 1272 nm. Even with atmospheric absorption and noise affecting the PRISMA spectrum, it is possible to perceive some diagnostic absorption bands that resemble those obtained in the laboratory.

Absorption near 2320 nm followed by a peak at 2350 nm may indicate that the spectrum captured by PRISMA corresponds to a luvisol, which is a shallow mineral soil with high clay activity, according to analysis by Meneses, Almeida and Baptista (2019).

The presence of clay can be inferred from the difference in intensity of the water absorption bands, where absorption at 1900 nm is observed to be much more intense compared to absorption at 1400 nm, an effect caused by the interference of clay minerals.

Meneses, Almeida and Baptista (2019) explain that in tropical countries, soils are found where physical weathering predominates over chemical weathering, and spectral absorptions result from the presence of primary minerals, metallic oxides, quartz and clays. In Brazil, they are predominantly located in the semi-arid region, which extends from Minas Gerais to Ceará, covering almost the entire Brazilian northeast.

Clay minerals are very important for rare earth mining because they absorb REE ions dissolved by weathering and concentrate these elements in what are called ionic clay deposits, which are the world's main source of rare earths, such as the Bayan Obo deposit, in China.

Bedini (2017) also points out that, in general, hyperspectral image analysis focuses on mapping alteration minerals, generated by weathering, and on detecting the host rock. Meneses, Almeida and Baptista (2019) add that, although the term may not seem appropriate, what is detected in hyperspectral scenes is a kind of "spectral mineralogy".

5. Machine Learning for recognition and mapping

Artificial Intelligence can be defined as the ability of computer systems to perform tasks that would require human intelligence, such as perceiving, learning, and solving problems through algorithms and data (Russell and Norvig, 2010).

Of the various existing AI techniques, Machine Learning stands out for its applications in different contexts and its ability to handle large amounts of data. This technique can be used in Artificial Neural Networks, models inspired by the structure and functioning of the human nervous system, where knowledge is acquired through the learning process and stored in the network's weights.

These network algorithms have been studied for spectral interpretation applications for several decades. Hippe (1991) states that algorithms of this type reflect a method of spectrum interpretation by correlation, which makes it possible to create an identification process based on attributes such as band location, intensity, and shape.

A systematic review of digital soil mapping showed evidence that Artificial Neural Network classifiers are more efficient than logistic regression models in predicting soil classes (Coelho et al, 2021).

The neural network's input data consists of laboratory-measured reflectance values comparable to those captured by the PRISMA Satellite, representing 239 wavelengths. Therefore, the decision was made to apply a Multilayer Perceptron (MLP) network for spectrum classification.

An MLP network represents the most rudimentary form of a feedforward neural network for class separation. Its basic architecture contains three layers: an input layer, which receives the dataset data; multiple hidden layers, which extract the necessary information from the data; and an output layer, which generates the final classification result.

Feedforward structure does not exhibit loop connections, it implements a static mapping that depends only on the inputs and their previous states, which are independent within the fully connected layers (Reed and Marks, 1999). This is useful for this application, since the data measured by PRISMA may eventually be incomplete.

The MLP architecture used can be seen in Figure 7. It has an input layer, where the 239 reflectance values are applied, hidden layers with ReLU activation and dropout functions, and an output layer of three neurons representing the three classes.

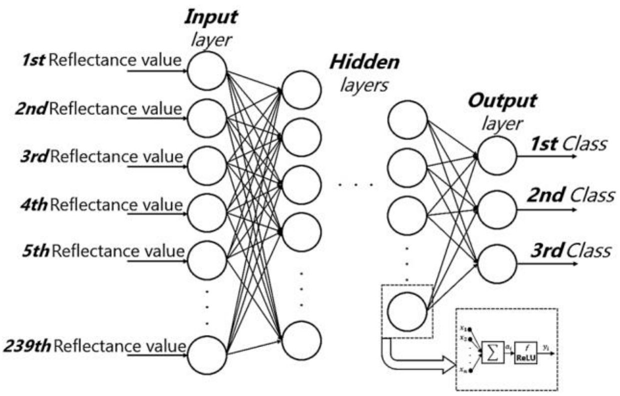

Figure 7. Architecture of the MLP neural network used.

The network has five hidden layers, one with 128 neurons and another with 64 neurons, interspersed with three dropout layers, where the rates were applied in a decreasing manner, starting at 0.4 and ending at 0.2.

The dataset was divided into: 70% for training, 15% for validation, and 15% for testing. In the training, the learning rate was set at 0.0005, with a batch of 64 and an early stopping with 15 epochs.

The training and validation curves showed significant fluctuations and some instability, resulting, at the end of 150 epochs, in an accuracy of 100%, as can be seen in the confusion matrix and the accuracy evolution graph in Figure 8.

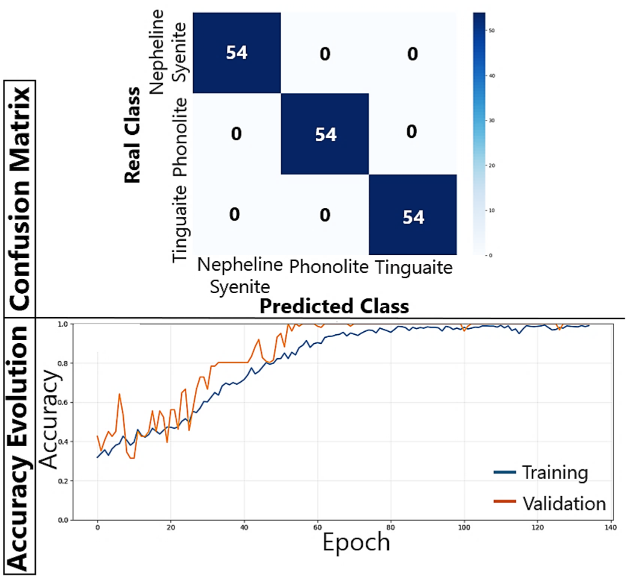

Figure 8. Confusion matrix and resulting accuracy evolution.

It should be taken into account that maximum accuracy was achieved due to the small dataset. Only three classes with little variation are insufficient for a robust modeling the network, making it necessary to expand and diversify the database.

Despite this, the model was able to classify the spectra satisfactorily, and was then applied to the hyperspectral image from the PRISMA Satellite in order to verify the occurrence of any of the classes in the image.

6. Materials and methodology

Reflectance measurements of the samples were performed at LaRaC, a laboratory of the Institute of Advanced Studies (IEAv), using a high-resolution ASD FieldSpec® 4 spectroradiometer.

The experimental setup of the sensor can be seen in Figure 9. The reflectance factor was measured using a Spectralon® plate as a reference. The fiber optic sensor, coupled to a biconvex lens used as a 1° Field-of-View (FOV) limiter, was positioned at nadir, with artificial illumination from a 75 W incandescent lamp at 15° from the sensor.

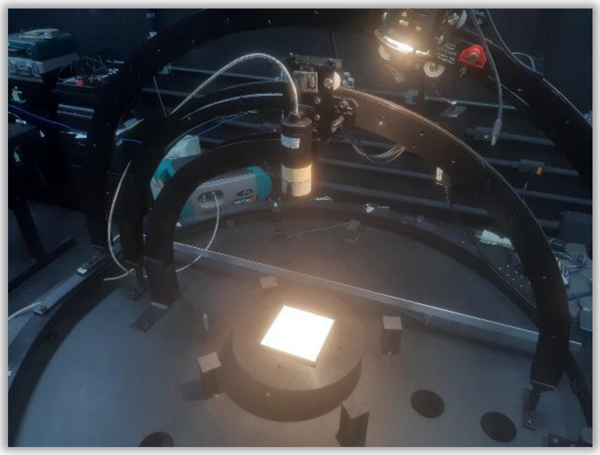

Figure 9. Experimental setup for carrying out the measurements.

The laboratory has a humidity and temperature control and monitoring system, set to 50% and 20°C, respectively. Before the measurements, the equipment remained powered on for a period of 30 minutes to allow for stabilization of the internal and ambient temperature.

The regolith samples were arranged in a 30 cm diameter aluminum mold and positioned perpendicularly 35 cm nadir distance from the sensor.

For each sample, 120 measurements were taken, and after each of these measurements, the sample was repositioned to be measured in its entirety, totaling 1080 measured spectra in the end.

After the measurements, the reflectance values obtained from each class of samples were sequentially arranged in spreadsheets, which formed the database used to train the neural network.

7. Classification Algorithm

An algorithm was developed using the Python programming language to read each pixel of the hyperspectral scene and apply the reflectance values of the associated spectra to the trained network model.

In order to reduce computational processing time, the calculation of Normalized Difference Vegetation Index (NDVI) and the comparison of spectra using the Spectral Angle Mapper (SAM) technique were made before classification by the neural network.

For the NDVI calculation, Equation 1 was used, which uses the reflectance values of near-infrared (NIR) and red wavelengths to determine whether the spectrum corresponds to soil or vegetation.

Values close to one represent dense and healthy vegetation, while values close to zero indicate bare soil or sparse, senescent vegetation.

$$NDVI = \frac{NIR - Red}{NIR + Red}, \tag{1}$$

where $NDVI$ = Normalized Difference Vegetation Index
NIR = NIR wavelength
Red = red wavelength

Equation 2, used to calculate SAM, was based on an algorithm for geological mapping of magmatic rocks, whose results were compared with data from orbital sensors of various resolutions (Girouard et al, 2004).

$$\alpha = cos^{-1}\left(\frac{\sum_{i=1}^{nb} t_i r_i}{\left(\sum_{i=1}^{nb} t_i{}^2\right)^{0.5}\left(\sum_{i=1}^{nb} r_i{}^2\right)^{0.5}}\right), \tag{2}$$

where α = spectral angle
nb = number of bands
t_i = test spectrum
r_i = reference spectrum

The SAM technique was used satisfactorily by Rocha and Souza Neto (2013) to map the spectral signature of bauxite in a 14-band multispectral scene. Therefore, verifying the SAM before classification brings greater reliability to the classification model.

As explained by Girouard et al (2004), the SAM algorithm is a fast way to check spectral similarity, in addition to suppressing the influence of shading factors to accentuate the reflectance characteristics of the target.

The integration between the spectral angle calculated by SAM and the class predicted by the neural network acts as a double check of the presented result, which adds greater reliability to the mapping algorithm.

The generation of the matrix of occurrence points of spectra similar to the REE samples by the algorithm took approximately 10 hours to complete.

The long time is due to the fact that the algorithm must access various directories within the hyperspectral image file whenever there is a possibility of occurrence, as previously determined by the NDVI and SAM calculations.

It is believed that the time can be reduced by using a computer system with greater memory capacity and by dividing the mapping into two individual parts, each covering 500 thousand pixels.

8. Results and discussion

Figure 10 shows the map generated by classifying the rare earth samples. The model classified 706 pixels as phonolite and 263 pixels as tinguaite, which represents approximately 0.1% of the total pixels in the image, equivalent to an area of 0.9 km².

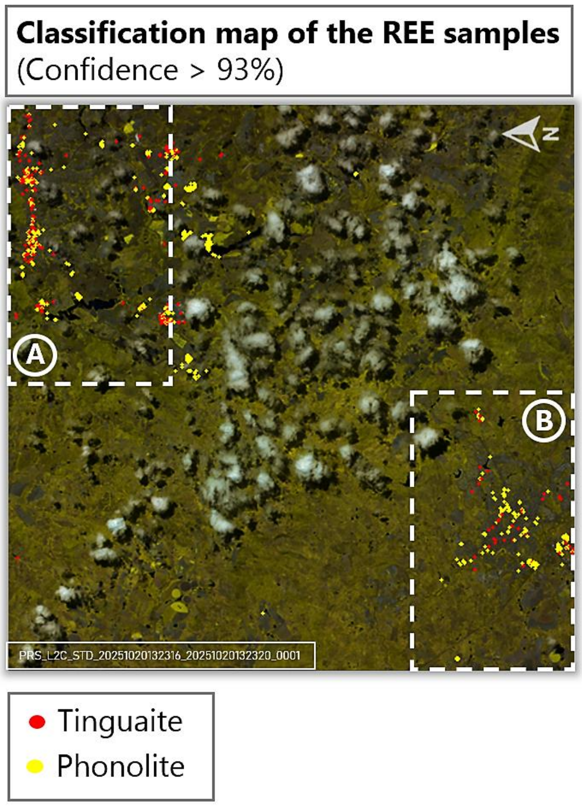

Figure 10. Classification map of the REE samples.

As can be seen on the map, the nepheline syenite samples were not classified into any pixel. This is because nepheline syenite is a type of rock that is not normally found on the surface, being present in deeper layers of the Earth's crust (Moraes and Seer, 2018).

Therefore, it is clear that the developed algorithm was able to distinguish the spectra well, classifying only those with 93% or more confidence.

The major difficulty presented by the model was the classification of the pixel spectra near clouds, especially thicker clouds that cover large areas.

A filter was added to the algorithm based on the cloud map provided by the PRISMA Product to avoid incorrect spectral classification.

In order to verify the classified areas, the map was divided into two regions based on the concentration of points for detailed analysis using Google Earth®.

Figure 11 shows region A, which concentrates the points in the urban area of Poços de Caldas. It was observed that many areas had their soil exposed due to land clearing for construction and vehicle traffic, as evidenced in image A4, which shows an open-air truck parking lot.

Figure 11. Detailed view of region A on the classification map.

In region A, it can be seen that the points were concentrated within a more densely populated urban area, with occurrences often occupying a single pixel, and these being close to houses, warehouses, streets, and lakes.

In region B, shown in Figure 12, there are more mining operations, which expose large areas of soil, occupying multiple pixels in the image, as can be seen in B1 and B3.

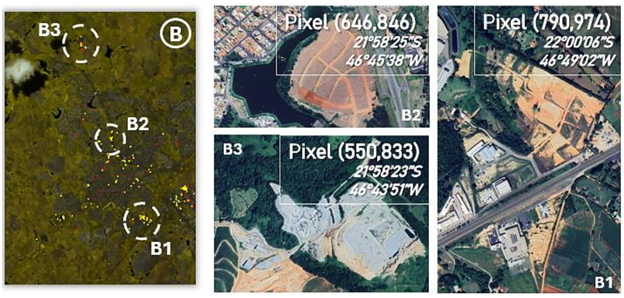

Figure 12. Detailed view of region B on the classification map.

It is clear that most of the points are located near urban areas, which have more exposed soil and less dense vegetation.

The proximity of the points is also noticeable, and because they are related to large-scale mining areas, they tend to occupy more pixels in the image.

The generated map showed that the 30 m GSD of the PRISMA Satellite proved efficient for mineral prospecting, in addition to demonstrating the robustness of the prediction model, which, combined with the SAM algorithm, was able to handle the noise present in the spectra due to atmospheric absorption and shading.

Figure 13 shows that, even with the presence of small clouds, the model was able to classify some of the drilling areas where the samples were collected[1].

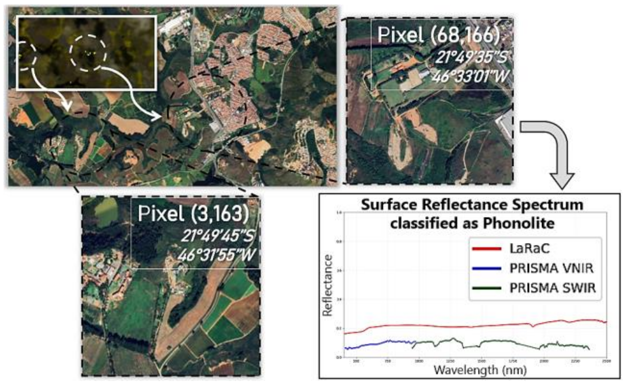

Figure 13. Areas of origin of the samples.

The region has demonstrated significant potential for the extraction of medium-sized REE near the surface. The notable presence of clay minerals indicates the economic viability for the implementation of mining projects.

Although useful, it is worth noting that visual validation does not replace a field analysis, which can quantitatively indicate the presence of minerals.

9. Conclusion

The demand for rare earth elements is expected to increase in the coming decades, driven by the energy transition and technological advancements. Consequently, developing efficient methods for identifying and mapping these elements becomes strategic for Brazil, which still has gaps in detailed national geological knowledge.

The results obtained demonstrated that the integration between hyperspectral remote sensing and machine learning is a viable way for classifying soils and rare earth rocks in the Poços de Caldas region. The model proved robust to atmospheric noise and shading, indicating its applicability in different scenarios and contexts, such as for classifying vegetation and organic matter, for example.

The study's limitations include the small size of the spectral database and the absence of quantitative field validation, aspects that can be improved in future work. Expanding the dataset, with the addition of more samples and geographic diversification, tends to increase the reliability of the algorithm and the scale of application of the methodology.

The proposed approach proves to be an additional tool for mineral exploration and geological mapping projects, capable of generating cost optimization and attracting new business to the mining sector in Brazil. Furthermore, the work contributes to reducing the geological knowledge gap in strategic regions, aligning with sustainable development policies and promoting better management of mineral resources.

Acknowledgements

This study was financed in part by the Coordenação de Aperfeiçoamento de Pessoal de Nível Superior - Brasil (CAPES) - Finance Code 001. We also thank Viridis Mining & Minerals for providing the samples, which enabled the creation of the spectral database and the training of the predictive model.

[1]As can be seen in: https://viridismining.com.au/project/colossus/

References

Abrão, A., 1994: *Química e tecnologia das terras-raras* [Chemistry and technology of rare earths]. CETEM/CNPq.

Badura, I., Dąbski, M., 2022: Reflectance spectroscopy in geology and soil sciences: literature review. *Quaestiones Geographicae*, 41(3), 157-167. https://doi.org/10.2478/quageo-2022-0031.

Bedini, E., 2017: The use of hyperspectral remote sensing for mineral exploration: a review. *Journal of Hyperspectral Remote Sensing*, 7, 189-211.

Cabral Neto, I., Abram, M., Almeida, R., Cunha, I., Silva, G., Silva, A., 2026. An overview of critical and strategic minerals potential of Brazil: 2026 edition, Geological Survey of Brazil. https://rigeo.sgb.gov.br/items/3e73d5fb-3cf7-4d62-885c-cf0d303a4bec.

Coelho, F., Giasson, E., Campos, A., Tiecher, T., Costa, J., Coblinski, J., 2021: Digital soil class mapping in Brazil: a systematic review. *Scientia Agricola*, 78, 1-11. https://doi.org/10.1590/1678-992X-2019-0227.

Genú, A., Demattê, J., 2012: Espectrorradiometria de solos e comparação com sensores orbitais [Soil spectroradiometry and comparison with orbital sensors]. *Bragantia*, 71, 82-89.

Girouard, G., Bannari, A., El Harti, A., Desrochers, A., 2004: Validated Spectral Angle Mapper Algorithm for Geological Mapping: Comparative Study between Quickbird and Landsat-TM. *ISPRS Proceedings*. https://www.isprs.org/proceedings/xxxv/congress/comm4/papers/432.pdf.

Goodenough, K., Deady, E., Beard, C., Broom-Fendley, S., Elliott, H., Berg, F., Öztürk, H., 2021: Carbonatites and Alkaline Igneous Rocks in Post-Collisional Settings: Storehouses of Rare Earth Elements. *Journal of Earth Science*, 32, 1332-1358. https://doi.org/10.1007/s12583-021-1500-5.

Heider, M., Siqueira, D., 2025: Novos potenciais das terras raras no Brasil [New potential of rare earths in Brazil]. In the Mine. https://www.inthemine.com.br/site/novos-potenciais-das-terras-raras-no-brasil-argilas-ionicas/.

Hippe, Z., 1991: *Artificial Intelligence in Chemistry: Structure elucidation and simulation of organic reactions*. Elsevier.

Italian Space Agency, 2020. PRISMA Products Specification Document.

Lapido-Loureiro, F., 2013: *O Brasil e a reglobalização da indústria das terras raras* [Brazil and the reglobalization of the rare earth industry]. CETEM/MCTI.

Mataveli, G., Morato, R., 2011: Estudo da expansão urbana do município de Poços de Caldas-MG e suas aplicações ambientais por meio de sensoreamento remoto e geoprocessamento [Study of the urban expansion of the municipality of Poços de Caldas-MG and its environmental applications through remote sensing and geoprocessing]. *Universidade Federal de Alfenas*.

Meneses, P., Almeida, T., Baptista, G., 2019: *Reflectância dos materiais terrestres: análise e interpretação* [Reflectance of terrestrial materials: analysis and interpretation]. Oficina de textos.

Moraes, L., Seer, H., 2018: *Terras Raras* [Rare Earths]. Companhia de Desenvolvimento de Minas Gerais.

Reed, R., Marks, R., 1999: *Neural Smithing: Supervised Learning in Feedforward Artificial Neural Networks*. MIT Press.

Rocha, B., Souza Neto, C., 2013: Geração de bibliotecas espectrais de bauxita brasileiros e exemplos de uso para a prospecção de minérios de alumínio por sensoriamento remoto orbital [Generation of spectral libraries of Brazilian bauxite and examples of use for prospecting aluminum ores by orbital remote sensing]. *XVI Simpósio Brasileiro de Sensoriamento Remoto*.

Russell, S., Norvig, P., 2010: *Artificial Intelligence*. Pearson Education.

Sgarbi, G., Schimdt, P., Santos, W., Silva, E., Gomes, S., Moraes, A., Gannam, L., 2007: *Petrografia macroscópica das rochas ígneas, sedimentares e metamórficas* [Macroscopic petrography of igneous, sedimentary, and metamorphic rocks]. Editora UFMG.